Hindawi Publishing Corporation
Advances in Materials Science and Engineering
Volume 2015, Article ID 235424, 8 pages
http://dx.doi.org/10.1155/2015/235424

Research Article

Evaluation of Interface Shear Strength Properties of Geogrid Reinforced Foamed Recycled Glass Using a Large-Scale Direct Shear Testing Apparatus

Arul Arulrajah,[1] Suksun Horpibulsuk,[1,2] Farshid Maghoolpilehrood,[1] Wisanukorn Samingthong,[2] Yan-Jun Du,[3] and Shui-Long Shen[4]

[1]*Department of Civil and Construction Engineering, Swinburne University of Technology, Melbourne, VIC 3122, Australia*
[2]*Suranaree University of Technology, Nakhon Ratchasima, Thailand*
[3]*Southeast University, Nanjing 210096, China*
[4]*State Key Laboratory of Ocean Engineering, School of Naval Architecture, Ocean, and Civil Engineering, Shanghai Jiao Tong University, Shanghai 200240, China*

Correspondence should be addressed to Arul Arulrajah; aarulrajah@swin.edu.au and Suksun Horpibulsuk; suksun@g.sut.ac.th

Received 2 June 2015; Revised 8 October 2015; Accepted 11 October 2015

Academic Editor: Luigi Nicolais

The interface shear strength properties of geogrid reinforced recycled foamed glass (FG) were determined using a large-scale direct shear test (DST) apparatus. Triaxial geogrid was used as a geogrid reinforcement. The geogrid increases the confinement of FG particles during shear; consequently the geogrid reinforced FG exhibits smaller vertical displacement and dilatancy ratio than FG at the same normal stress. The failure envelope of geogrid reinforced FG, at peak and critical states, coincides and yields a unique linear line possibly attributed to the crushing of FG particles and the rearrangement of crushed FG after peak shear state. The interface shear strength coefficient α is approximately constant at 0.9. This value can be used as the interface parameter for designing a reinforced embankment and mechanically stabilized earth (MSE) wall when FG is used as a lightweight backfill and triaxial geogrid is used as an extensible earth reinforcement. This research will enable FG, recently assessed as suitable for lightweight backfills, to be used together with geogrids in a sustainable manner as a lightweight MSE wall. The geogrid carries tensile forces, while FG reduces bearing stresses imposed on the in situ soil. The use of geogrid reinforced FG is thus significant from engineering, economical, and environmental perspectives.

1. Introduction

Lightweight fill materials are increasingly being used as construction materials in civil engineering applications. The prime purpose for lightweight fill materials is to reduce the weight of fills, thereby mitigating excessive settlements and bearing failures [1, 2]. Lightweight fill materials include expanded polystyrene [3–8], lightweight cellular cemented clays [1, 2, 9–11], and tires [12–15].

Reuse applications for industrial waste materials are increasingly being sought, inclusive of demolition wastes [16–21], municipal solid wastes [22, 23], calcium carbide residue [1, 24], and other forms of commercial and industrial wastes [21, 25–32]. The interface shear strength properties of residual soil and construction and demolition materials with geosynthetics using large-scale direct shear tests have been undertaken in recent years [33–35].

In recent years, there has been interest in the development of lightweight foamed materials with the usage of waste materials in engineering applications [36, 37]. Recycled waste glass is a viable construction material for embankments and pavement subbases [21, 28, 38–41], footpath bases [42], and problematic soil treatment [43, 44]. The usage of foamed glass (FG) is still in its infancy, with limited works to date in the production of ceramics [45, 46] and insulating applications [46–52]. Engineering and environmental evaluation of FG has recently been assessed to be suitable as a lightweight embankment fill material [38, 39].

The focus of this research is to extend the research of FG usage as a lightweight fill material by evaluating the interface shear strength properties when reinforced with geogrids. Due to high tensile strength of geogrid, the overall shear strength of the geogrid reinforced FG would be improved. The geogrids are commonly used as extensible earth reinforcement for embankment and mechanically stabilized earth wall in Asia [53, 54]. As a reinforced embankment and a mechanically stabilized earth (MSE) wall, the interface mechanism of geogrid and FG is vital for stability analysis. A large-scale direct shear box in this research is used to investigate interface mechanism of geogrid and FG, which has not been previously investigated. The outcomes will enable FG to be used as a lightweight backfill in combination of geogrid as reinforcement for the construction of sustainable lightweight reinforced embankments and MSE walls on soft clay deposits in coastal regions. The innovative usage of lightweight FG material, such as in combination with geogrid reinforcement, is significant from engineering and environmental perspectives.

2. Materials and Methods

2.1. Foamed Glass (FG) and Geogrid Reinforcement. FG for this research was obtained from a supplier in Melbourne, Australia. The FG was manufactured by firstly grounding glass collected from the municipal waste stream. The recycled glass was fired with mineral additives in a furnace at temperatures up to 950 degrees Celsius. The recycled glass, comprising 98% ground recycled glass and 2% mineral additives, then foams and was removed from the furnace at which point it cooled down quickly forming low weight FG aggregates of up to 40 mm in size [38, 39]. The FG aggregates are comprised of vesiculars, due to the presence of air that forms small voids during the production process. Figure 1 shows a close-up photo of the FG material.

Particle size distribution curves of FG are shown in Figure 2. The material comprises essentially gravel and sand sized particles. FG is gap graded, with two major grain size ranges, 0.08–0.3 mm and 10–35 mm, and the average grain size of 18 mm. The particle density of the coarse FG was 4.5 kN/m^3 while the particle density of the fine FG was 14.8 kN/m^3, almost three times higher than that of the coarse particle density. The water absorption of fine particles was low of 0.3%, while the coarse particle water absorption was high of 60%. The pH value for FG was found to be 10.5, which is in the alkali range, similar to that for typical construction and demolition materials including recycled concrete aggregate, crushed brick, and reclaimed asphalt pavement, which have been reported to have pH values in the range of 8–12 [16, 35]. Organic materials were not present in FG.

The CBR values of FG were 9–12%, which are within the local road authority specification requirements (typically a minimum of 2–5%) for a structural fill material in road embankments [55]. The LA abrasion value was 90%, which exceeds the maximum LA abrasion value of 40% typically specified for pavement base/subbase applications. The LA and CBR results for FG indicate that the material is suitable for embankment fills but is not suitable for higher load applications unless it is reinforced by geosynthetics.

Figure 1: Close-up photo of FG.

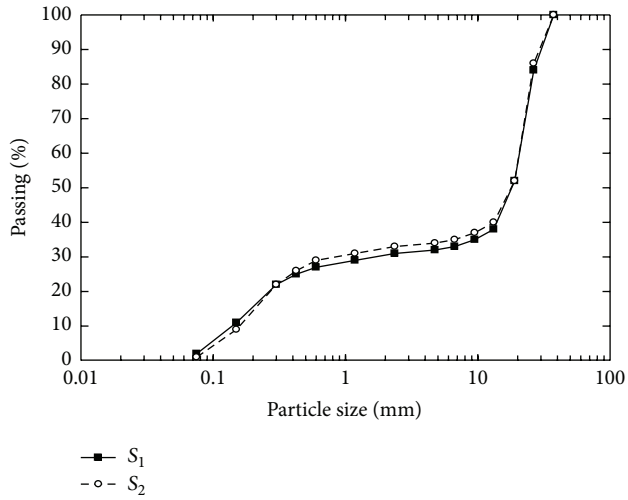

Figure 2: Gradation curves for FG.

A commercially available triaxial geogrid used to reinforce FG in this study is made of polypropylene and has an aperture size of 46 × 46 × 46 mm and unit weight of 0.25 kg/m^2. The triaxial geogrid has a higher tensile strength than biaxial geogrids and has in recent years become increasingly available commercially for various civil engineering applications. The mechanical properties of the triaxial geogrid used had an ultimate tensile strength of 32 kN/m and a failure strain of 18%, as determined from a tensile strength test undertaken using a 500 kN capacity universal testing machine, with geosynthetic grips.

2.2. Methods of Testing. A large-scale direct shear test (DST) apparatus, with shear boxes measuring 305 mm in length, 305 mm in width, and 204 mm in depth, was used to evaluate the interface shear strength response of FG with geogrid reinforcement. Control tests were undertaken on unreinforced FG aggregates to compare the effect of the geogrid reinforced FG with unreinforced FG. The tests were conducted as per ASTM [56].

The large-scale DST apparatus has two boxes: a fixed upper box and a moveable lower box. Initially, the lower

Figure 3: Shear box after completion of an interface shear test.

and upper boxes were clamped when preparing samples for the tests. The samples were compacted in the shear box in three layers by using hand tamping with a plastic hammer to attain the maximum dry density of 290 kg/m^3 obtained from the vibratory table method. The samples were submerged prior to the commencement of the consolidation stage, by filling the entire lower shear box and half of the upper shear box with water. The consolidation stage was for 12 hours with three normal stress levels of 10 kPa, 20 kPa, and 40 kPa. When the consolidation stage for the tests was completed, the connection between the lower and upper boxes was released, which provided an approximate 2 mm gap between the upper and lower boxes for friction minimization. The shearing stage of the test was next conducted under the same normal stress levels of 10 kPa, 20 kPa, and 40 kPa. A shear displacement rate of 0.025 mm/min was maintained throughout the shearing stage. The horizontal displacements, vertical displacements, and shear stresses were recorded. The tests were terminated once the horizontal shear displacement reached approximately 75 mm. The room temperature was maintained at 20 ± 1°C. The shear strength of FG and interface shear strength of geogrid reinforced FG from the DST tests were obtained from the shear stress and horizontal displacement output graphs. Figure 3 shows the shear box after completion of shearing test, showing the geogrid, which is gripped at the outer edge of the lower shear box.

3. Results and Discussions

Figure 4 presents the DST results of FG. FG shows strain-hardening behavior in shear stress versus horizontal displacement relationship. For a particular normal stress, the shear stress increases with horizontal displacement and the peak shear stress is reached at approximately 50 mm displacement. The shear stress is essentially constant with increasing displacement until the end of test at 75 mm. With increasing

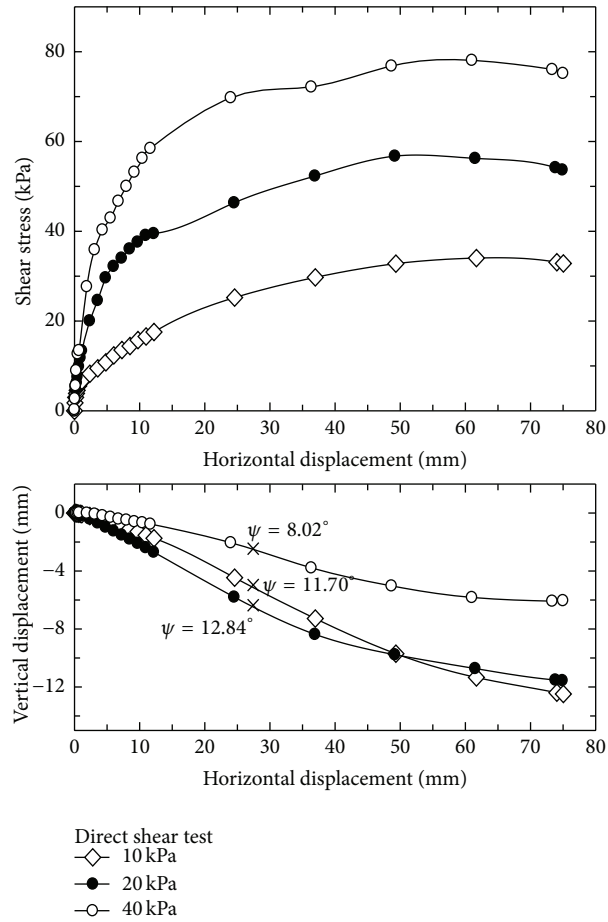

Figure 4: DST test results of FG.

normal stress, the peak shear stress and the shear stiffness increase.

FG was found to exhibit completely dilatant behavior in vertical displacement and horizontal displacement relationship for all normal stresses tested while exhibiting strain-hardening behavior in shear stress versus displacement relationship. This shear response is in contradiction to the typical shear response for typical coarse-grained geomaterial, where dilatant behavior is associated with strain-softening behavior and the peak shear strengths are attained at the maximum dilatancy ratio (slope of the relationship between vertical displacement and horizontal displacement). The increase in shear stress even after the maximum dilatancy ratio (strain hardening) is caused by the rearrangement of crushed particles (fine crushed particles are driven into the voids or pores). The shear response of FG is found to be similar to that of recycled glass cullets that has been used as aggregates in pavements and designated as having dilatancy associated strain-hardening response [25, 33, 40].

The vertical displacement versus horizontal displacement relationships are almost the same for low normal stresses of 10 and 20 kPa. The relationship for 40 kPa normal stress diverts from the relationships for the low normal stresses, indicating lower maximum dilatant displacement of 6 mm (half of the dilatant displacement for normal stresses of 10 and 20 kPa).

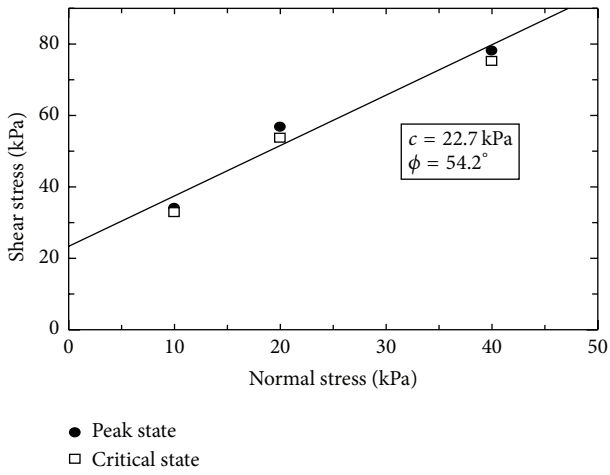

Figure 5: Shear strength failure envelope for unreinforced FG.

The maximum dilatancy ratios (ψ) for all the normal stresses are found at approximately the same horizontal displacement of 23 mm. The maximum dilatancy ratio decreases and shear stiffness increases as the normal stress increases due to higher confinement. The ψ values are 12.8°, 11.7°, and 8.0° for normal stress of 10, 20, and 40 kPa, respectively.

The cohesion and friction angle based on the Mohr-Coulomb failure criterion at peak and critical (end of test) states are shown in Figure 5. It is evident that the peak and critical state shear stresses are essentially the same at the same normal stresses and yield a unique failure envelope having cohesion of 22.7 kPa and friction angle of 54.2 degrees. This high friction angle meets the shear strength property requirement for lightweight fill materials and is consistent with that of a dense gravel material. The high shear strength parameters with strain-hardening response indicate that this material is strong and ductile, which can resist large deformation and can be used as backfill of MSE wall according to AASHTO specifications.

Figure 6 presents the interface shear response of the geogrid reinforced FG. The geogrid reinforced FG exhibits strain-hardening behavior in interface shear stress versus horizontal displacement relationship especially for normal stresses greater than 10 kPa, which is similar to FG. For a particular normal stress, the peak interface shear stress is found at approximately 40–50 mm displacement and then the interface shear stress tends to be constant. The peak interface shear stress and interface shear stiffness increase with increasing normal stress. The vertical displacement versus horizontal relationship is dependent upon the applied normal stress; that is, the higher normal stress results in the lower dilatant displacement. Similar to the shear behavior of FG, the dilatant behavior in vertical displacement versus horizontal relationship is associated with strain-hardening behavior in interface shear stress versus horizontal displacement relationship. This response is in contradiction to the typical interface shear response for geogrid reinforced coarse-grained material.

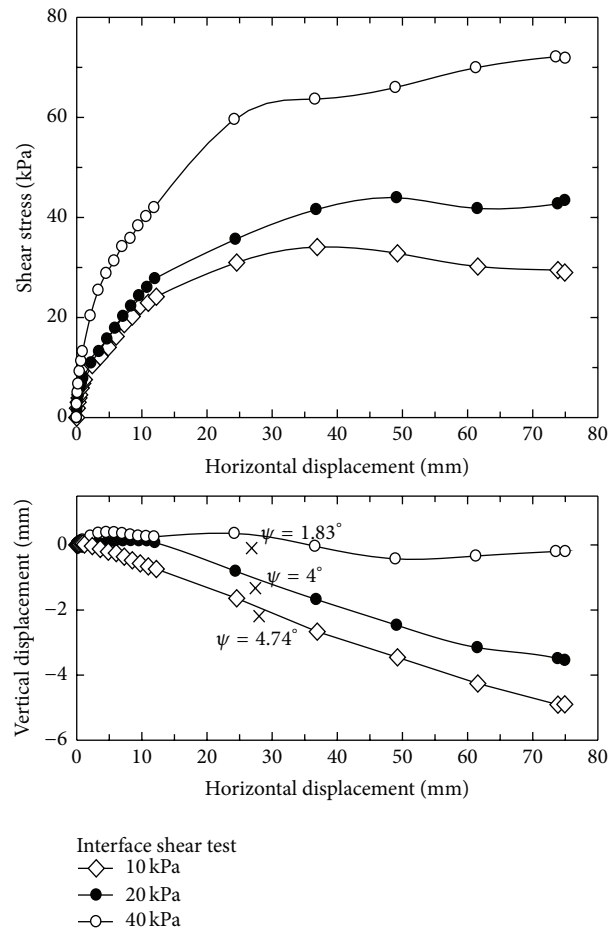

Figure 6: DST test results of geogrid reinforced FG.

It is found that the peak interface shear stress of geogrid reinforced FG is slightly lower than the peak shear stress of FG, whereas the interface shear stress of geosynthetics reinforced backfill material is commonly significantly lower than the shear strength of backfill material. The high interface shear stress can be attributed to the geogrid having a large aperture size of greater than the average grain size of FG, about 2.6 times and having high tensile strength and stiffness. The geogrid prevents the movement of FG particles; hence the FG particles reorientate around each other, as the FG particles are unable to slide on the geogrid. Consequently, the interface shear strength is mainly contributed from the highly confined soil to soil interaction.

The effect of confinement is also observed by the stiffness of the interface shear stress versus displacement of the geogrid reinforced FG, which is higher than that of the shear stress versus displacement of FG (comparing Figures 4–6). For the same applied shear stress, the shear displacement of the geogrid reinforced FG is smaller than that of FG. It is noted that, at the same shear displacement, the dilatant (vertical) displacement of geogrid reinforced FG is significantly lower than that of FG, especially at high normal stress. For instance, at 40 kPa normal stress, the end of test vertical displacement is −0.2 mm (negative sign indicates expansion)

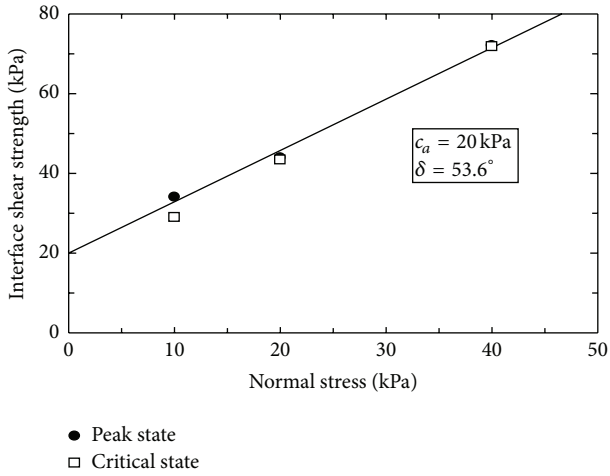

Figure 7: Interface stress failure envelope for geogrid reinforced FG.

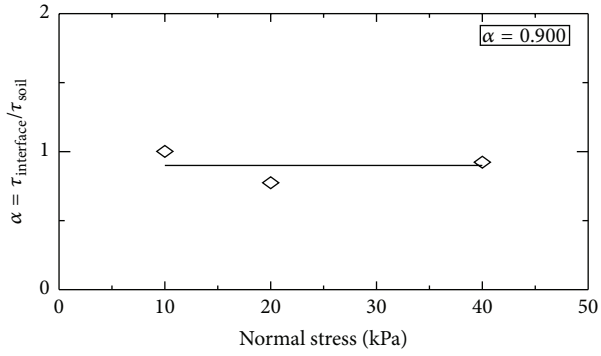

Figure 8: Relationship between coefficient of soil-reinforcement friction α and normal stress.

for geogrid reinforced FG while it is −6 mm for FG. This increase in confinement by geogrid also reduces the ψ values; that is, $\psi = 4.7^\circ$, 4.0°, and 1.8° for normal stress of 10, 20, and 40 kPa, respectively.

The interface shear strength parameters for geogrid reinforced FG are determined based on the Mohr-Coulomb failure criterion and shown in Figure 7. Similar to the failure envelope of FG, the interface failure envelope at peak and critical states coincides and yields a unique set of interface shear strength parameters: adhesion (c_a) = 20 kPa and interface friction angle (δ) = 53.6 degrees. These interface shear strength parameters of the geogrid reinforced FG are slightly lower than the shear strength parameters of the unreinforced FG.

FG having low tensile strengths can fail by tensile stress due to the traffic load. When the geogrid reinforcement is introduced, the modes of failure of the composite material will be by either tension (or rupture) or slip failure. The rupture failure happens when tensile stress in the geogrid exceeds its tensile strength while the slip failure, which is movement of the FG on the geogrid reinforced FG, is controlled by the interface shear strength. The interface between geogrid and FG can be expressed as the interface shear strength coefficient [34, 35]. The interface shear strength coefficient is obtained from the following equation:

$$\alpha = \frac{\tau_{\text{interface}}}{\tau_f}, \tag{1}$$

where α is interface shear strength coefficient and $\tau_{\text{interface}}$ and τ_f are the interface shear strength between geogrid and FG and shear strength of FG, respectively. It is found that α value varies in a narrow band and can be considered as constant of 0.9 based on the linear regression analysis (Figure 8). This value can be used as the interface parameter for reinforced embankment and MSE wall when FG is used as a lightweight backfill and triaxial geogrids are used for earth reinforcement. The interface shear strength coefficient is found to be close to values reported previously for geogrid reinforced recycled asphalt pavement (0.88), crushed brick (0.79), and recycled concrete (0.71) [33]. The advantage of this lightweight MSE over the conventional MSE wall is the usage of recycled waste and the low bearing stress on the foundation, which will result in small settlement. This lightweight MSE wall can be applied on soft clay deposits in coastal regions. The pullout tests on geogrid embedded in FG are required for the examination of internal stability against pullout failure and can be a future research.

4. Conclusions

A large-scale DST apparatus was used to determine the interface shear strength properties of geogrid reinforced FG. Tests were undertaken on each of the respective FG aggregates when reinforced with triaxial geogrids. Tests were also undertaken on unreinforced FG aggregates for comparisons. The key conclusion is drawn as follows:

(1) Even though the FG is classified as coarse-grained material, the direct shear response of FG under drained condition is in contradiction to the typical shear response for typical coarse-grained geomaterial, where dilatant behavior is associated with strain-softening behavior and the peak shear strengths are attained at the maximum dilatancy ratio. This difference can be attributed to the breakage of FG particles during shear. The peak and critical failure envelopes are found to coincide and are represented by a linear line. With high strength parameters, FG can be used as lightweight backfill for MSE wall.

(2) The geogrid reinforced FG exhibits strain-hardening behavior in interface shear stress versus horizontal displacement relationship, which is similar to FG. The interface shear strength and interface shear stiffness increase while the dilatant displacement reduces with increasing normal stress. The interface shear strength of geogrid reinforced FG is slightly lower than the shear strength of FG. The high interface shear strength of geogrid reinforced FG can be attributed to the geogrid having a large aperture size of greater than the average grain size of FG of about 2.6 times and a high tensile strength. Consequently, the interface

strength is contributed by highly confined soil to soil interaction.

(3) The geogrid increases the confinement and prevents shear and vertical displacement of FG. For the same applied shear stress, the shear displacement of the geogrid reinforced FG is smaller than FG. At the same shear displacement, the dilatant displacement of geogrid reinforced FG is significantly lower than that of FG, especially at high normal stress. Similar to the failure envelope of FG, the interface failure envelope at peak and critical states coincides and yields a unique set of interface shear strength parameters.

(4) The interface shear strength coefficient α commonly used to express interface behavior is investigated in this paper for geogrid and FG interaction. The constant α of 0.9 can be used as the interface parameter for designing reinforced embankment and MSE wall when FG is used as a lightweight backfill and triaxial geogrid is used as earth reinforcement.

(5) This research will enable FG, which has been recently assessed as suitable for lightweight backfill, to be used in combination with geogrid in a sustainable manner as a lightweight MSE wall. The geogrid carries the tensile force due to dead and live loads on the reinforced embankment and MSE wall while FG causes low bearing stress on foundation. This lightweight MSE wall is applicable particularly for soft clay deposits in coastal regions. The use of geogrid reinforced FG is thus significant from engineering, economical, and environmental perspectives.

Conflict of Interests

The authors declare that there is no conflict of interests regarding the publication of this paper.

Acknowledgments

The second and fourth authors are grateful for the financial support from the Thailand Research Fund under the TRF Senior Research Scholar program Grant no. RTA5680002, Suranaree University of Technology, and the Office of Higher Education Commission under NRU Project of Thailand. The fifth author is grateful for the financial support from National Natural Science Foundation of China (Grant nos. 51278100 and 41472258).

References

[1] S. Horpibulsuk, V. Munsrakest, A. Udomchai, A. Chinkulkijniwat, and A. Arulrajah, "Strength of sustainable non-bearing masonry units manufactured from calcium carbide residue and fly ash," *Construction and Building Materials*, vol. 71, pp. 210–215, 2014.

[2] S. Horpibulsuk, A. Wijitchot, A. Nerimitknornburee, S. L. Shen, and C. Suksiripattanapong, "Factors influencing unit weight and strength of lightweight cemented clay," *Quarterly Journal of Engineering Geology and Hydrogeology*, vol. 47, no. 1, pp. 101–109, 2014.

[3] A. Athanasopoulos - Zekkos, K. Lamote, and G. A. Athanasopoulos, "Use of EPS geofoam compressible inclusions for reducing the earthquake effects on yielding earth retaining structures," *Soil Dynamics and Earthquake Engineering*, vol. 41, pp. 59–71, 2012.

[4] A. Deng and Y. Xiao, "Measuring and modeling proportion-dependent stress-strain behavior of EPS-sand mixture," *International Journal of Geomechanics*, vol. 10, no. 6, pp. 214–222, 2010.

[5] O. L. Ertugrul and A. C. Trandafir, "Reduction of lateral earth forces acting on rigid nonyielding retaining walls by EPS geofoam inclusions," *Journal of Materials in Civil Engineering*, vol. 23, no. 12, pp. 1711–1718, 2011.

[6] L.-K. Lin, L.-H. Chen, and R. H. L. Chen, "Evaluation of geofoam as a geotechnical construction material," *Journal of Materials in Civil Engineering*, vol. 22, no. 2, pp. 160–170, 2010.

[7] A. C. Trandafir and B. A. Erickson, "Stiffness degradation and yielding of EPS geofoam under cyclic loading," *Journal of Materials in Civil Engineering*, vol. 24, no. 1, pp. 119–124, 2012.

[8] Y. Zou, C. J. Leo, and H. Wong, "Time dependent viscoelastic behaviour of Eps geofoam," *Applied Mechanics and Materials*, vol. 330, pp. 1095–1099, 2013.

[9] A. Neramitkornburi, S. Horpibulsuk, S. L. Shen, A. Arulrajah, and M. M. Disfani, "Engineering properties of lightweight cellular cemented clay-fly ash material," *Soils and Foundations*, vol. 55, no. 2, pp. 471–783, 2015.

[10] A. Neramitkornburi, S. Horpibulsuk, S. L. Shen, A. Chinkulkijniwat, A. Arulrajah, and M. M. Disfani, "Durability against wetting-drying cycles of sustainable lightweight cellular cemented construction material comprising clay and fly ash wastes," *Construction and Building Materials*, vol. 77, pp. 41–49, 2015.

[11] C. Teerawattanasuk, P. Voottipruex, and S. Horpibulsuk, "Mix design charts for lightweight cellular cemented Bangkok clay," *Applied Clay Science*, vol. 104, pp. 318–323, 2015.

[12] V. Cecich, L. Gonzales, A. Hoisaeter, J. Williams, and K. Reddy, "Use of shredded tires as lightweight backfill material for retaining structures," *Waste Management and Research*, vol. 14, no. 5, pp. 433–451, 1996.

[13] I. F. Hodgson, S. P. Beales, and M. J. Curd, "Use of tyre bales as lightweight fill for the A421 improvements scheme near Bedford, UK," *Geological Society Engineering Geology Special Publication*, vol. 26, no. 1, pp. 101–108, 2012.

[14] S. N. M. Tafreshi, G. T. Mehrjardi, and A. R. Dawson, "Buried pipes in rubber-soil backfilled trenches under cyclic loading," *Journal of Geotechnical and Geoenvironmental Engineering*, vol. 138, no. 11, pp. 1346–1356, 2012.

[15] A. Nakhaei, S. M. Marandi, S. Sani Kermani, and M. H. Bagheripour, "Dynamic properties of granular soils mixed with granulated rubber," *Soil Dynamics and Earthquake Engineering*, vol. 43, pp. 124–132, 2012.

[16] A. Arulrajah, J. Piratheepan, M. M. Disfani, and M. W. Bo, "Geotechnical and geoenvironmental properties of recycled construction and demolition materials in pavement subbase applications," *Journal of Materials in Civil Engineering*, vol. 25, no. 8, pp. 1077–1088, 2013.

[17] L. R. Hoyos, A. J. Puppala, and C. A. Ordonez, "Characterization of cement-fiber-treated reclaimed asphalt pavement aggregates: preliminary investigation," *Journal of Materials in Civil Engineering*, vol. 23, no. 7, pp. 977–989, 2011.

[18] A. J. Puppala, L. R. Hoyos, and A. K. Potturi, "Resilient moduli response of moderately cement-treated reclaimed asphalt pavement aggregates," *Journal of Materials in Civil Engineering*, vol. 23, no. 7, pp. 990–998, 2011.

[19] R. Taha, A. Al-Harthy, K. Al-Shamsi, and M. Al-Zubeidi, "Cement stabilization of reclaimed asphalt pavement aggregate for road bases and subbases," *Journal of Materials in Civil Engineering*, vol. 14, no. 3, pp. 239–245, 2002.

[20] M. A. Rahman, A. Arulrajah, J. Piratheepan, M. W. Bo, and M. A. Imteaz, "Resilient modulus and permanent deformation responses of geogrid-reinforced construction and demolition materials," *Journal of Materials in Civil Engineering*, vol. 26, no. 3, pp. 512–519, 2014.

[21] J. Wartman, D. G. Grubb, and A. S. M. Nasim, "Select engineering characteristics of crushed glass," *Journal of Materials in Civil Engineering*, vol. 16, no. 6, pp. 526–539, 2004.

[22] K. R. Reddy, H. Hettiarachchi, N. S. Parakalla, J. Gangathulasi, and J. E. Bogner, "Geotechnical properties of fresh municipal solid waste at Orchard Hills Landfill, USA," *Waste Management*, vol. 29, no. 2, pp. 952–959, 2009.

[23] D. Zekkos, J. D. Bray, E. Kavazanjian Jr. et al., "Unit weight of municipal solid waste," *Journal of Geotechnical and Geoenvironmental Engineering*, vol. 132, no. 10, pp. 1250–1261, 2006.

[24] C. Phetchuay, S. Horpibulsuk, C. Suksiripattanapong, A. Chinkulkijniwat, A. Arulrajah, and M. M. Disfani, "Calcium carbide residue: alkaline activator for clay-fly ash geopolymer," *Construction and Building Materials*, vol. 69, pp. 285–294, 2014.

[25] A. Arulrajah, M. M. Disfani, S. Horpibulsuk, C. Suksiripattanapong, and N. Prongmanee, "Physical properties and shear strength responses of recycled construction and demolition materials in unbound pavement base/subbase applications," *Construction and Building Materials*, vol. 58, pp. 245–257, 2014.

[26] M. M. Disfani, A. Arulrajah, H. Haghighi, A. Mohammadinia, and S. Horpibulsuk, "Flexural beam fatigue strength evaluation of crushed brick as a supplementary material in cement stabilized recycled concrete aggregates," *Construction and Building Materials*, vol. 68, pp. 667–676, 2014.

[27] Y.-J. Du, N.-J. Jiang, S.-Y. Liu, F. Jin, D. N. Singh, and A. J. Puppala, "Engineering properties and microstructural characteristics of cement-stabilized zinc-contaminated kaolin," *Canadian Geotechnical Journal*, vol. 51, no. 4, pp. 289–302, 2014.

[28] D. G. Grubb, P. M. Gallagher, J. Wartman, Y. Liu, and M. Carnivale III, "Laboratory evaluation of crushed glass-dredged material blends," *Journal of Geotechnical and Geoenvironmental Engineering*, vol. 132, no. 5, pp. 562–576, 2006.

[29] A. Kampala, S. Horpibulsuk, A. Chinkullijniwat, and S.-L. Shen, "Engineering properties of recycled calcium carbide residue stabilized clay as fill and pavement materials," *Construction and Building Materials*, vol. 46, pp. 203–210, 2013.

[30] A. Kampala, S. Horpibulsuk, N. Prongmanee, and A. Chinkulkijniwat, "Influence of wet-dry cycles on compressive strength of calcium carbide residue-fly ash stabilized clay," *Journal of Materials in Civil Engineering*, vol. 26, no. 4, pp. 633–643, 2014.

[31] T. L. Landris, "Recycled glass and dredged materials," Engineer Research and Development Center Report ERDC TN-DOER-T8, US Army Corps of Engineers, Vicksburg, Miss, USA, 2007.

[32] M. A. Rahman, M. A. Imteaz, A. Arulrajah, J. Piratheepan, and M. M. Disfani, "Recycled construction and demolition materials in permeable pavement systems: geotechnical and hydraulic characteristics," *Journal of Cleaner Production*, vol. 90, pp. 183–194, 2015.

[33] A. Arulrajah, M. A. Rahman, J. Piratheepan, M. W. Bo, and M. A. Imteaz, "Evaluation of interface shear strength properties of geogrid-reinforced construction and demolition materials using a modified large-scale direct shear testing apparatus," *Journal of Materials in Civil Engineering*, vol. 26, no. 5, pp. 974–982, 2014.

[34] F. B. Ferreira, C. S. Vieira, and M. L. Lopes, "Direct shear behaviour of residual soil-geosynthetic interfaces—influence of soil moisture content, soil density and geosynthetic type," *Geosynthetics International*, vol. 22, no. 3, pp. 257–272, 2015.

[35] C. S. Vieira and P. M. Pereira, "Interface shear properties of geosynthetics and construction and demolition waste from large-scale direct shear tests," *Geosynthetics International*, 2015.

[36] P. Jana, V. Fierro, and A. Celzard, "Ultralow cost reticulated carbon foams from household cleaning pad wastes," *Carbon*, vol. 62, pp. 517–520, 2013.

[37] G. Wang, L. Sha, and F. Jin, "Study on the strength properties and failure mode of recycled sludge lightweight soil," *Applied Mechanics and Materials*, vol. 275–277, pp. 1281–1284, 2013.

[38] A. Arulrajah, M. M. Disfani, F. Maghoolpilehrood et al., "Engineering and environmental properties of foamed recycled glass as a lightweight engineering material," *Journal of Cleaner Production*, vol. 94, pp. 369–375, 2015.

[39] A. Arulrajah, M. M. Disfani, H. Haghighi, A. Mohammadinia, and S. Horpibulsuk, "Modulus of rupture evaluation of cement stabilized recycled glass/recycled concrete aggregate blends," *Construction and Building Materials*, vol. 84, pp. 146–155, 2015.

[40] A. Arulrajah, M. M. Y. Ali, M. M. Disfani, and S. Horpibulsuk, "Recycled-glass blends in pavement base/subbase applications: laboratory and field evaluation," *Journal of Materials in Civil Engineering*, vol. 26, no. 7, Article ID 04014025, 2014.

[41] M. A. Rahman, M. Imteaz, A. Arulrajah, and M. M. Disfani, "Suitability of recycled construction and demolition aggregates as alternative pipe backfilling materials," *Journal of Cleaner Production*, vol. 66, pp. 75–84, 2014.

[42] A. Arulrajah, M. M. Y. Ali, M. M. Disfani, J. Piratheepan, and M. W. Bo, "Geotechnical performance of recycled glass-waste rock blends in footpath bases," *Journal of Materials in Civil Engineering*, vol. 25, no. 5, pp. 653–661, 2013.

[43] F. Ahmad, D. Mujah, H. Hazarika, and A. Safari, "Assessing the potential reuse of recycled glass fibre in problematic soil applications," *Journal of Cleaner Production*, vol. 35, pp. 102–107, 2012.

[44] D. Mujah, F. Ahmad, H. Hazarika, and A. Safari, "Evaluation of the mechanical properties of recycled glass fibers-derived three dimensional geomaterial for ground improvement," *Journal of Cleaner Production*, vol. 52, pp. 495–503, 2013.

[45] H. R. Fernandes, D. U. Tulyaganov, and J. M. F. Ferreira, "Production and characterisation of glass ceramic foams from recycled raw materials," *Advances in Applied Ceramics*, vol. 108, no. 1, pp. 9–13, 2009.

[46] I. Ponsot and E. Bernardo, "Self glazed glass ceramic foams from metallurgical slag and recycled glass," *Journal of Cleaner Production*, vol. 59, pp. 245–250, 2013.

[47] G. Bumanis, D. Bajare, J. Locs, and A. Korjakins, "Alkali-silica reactivity of foam glass granules in structure of lightweight concrete," *Construction and Building Materials*, vol. 47, pp. 274–281, 2013.

[48] H. W. Guo, Z. X. Mo, P. Liu, and D. N. Gao, "Improved mechanical property of foam glass composites toughened by mullite fiber," *Applied Mechanics and Materials*, vol. 357–360, pp. 1370–1373, 2013.

[49] L. K. Kazantseva, "Particulars of foam glass manufacture from zeolite-alkali batch," *Glass and Ceramics*, vol. 70, pp. 277–281, 2013.

[50] K. Pawanawichian, W. Thiemsorn, A. Wannagon, and P. Laoarun, "Fabrication of glass foams from industrial wastes used as insulating board," *Advanced Materials Research*, vol. 770, pp. 205–208, 2013.

[51] Q. Wang, N. Wang, Z. Y. Ding, and T. J. Wu, "Influences of firing process system on foam glass properties," *Advanced Materials Research*, vol. 721, pp. 258–261, 2013.

[52] L. Wu, Y. H. Zhao, R. F. Chen et al., "Effect of foaming temperature and holding time on foam glass," in *Advances in Manufacturing Science and Engineering*, pp. 897–900, 2013.

[53] S. Horpibulsuk and A. Niramitkornburee, "Pullout resistance of bearing reinforcement embedded in sand," *Soils and Foundations*, vol. 50, no. 2, pp. 215–226, 2010.

[54] C. Suksiripattanapong, S. Horpibulsuk, A. Chinkulkijniwat, and J. C. Chai, "Pullout resistance of bearing reinforcement embedded in coarse-grained soils," *Geotextiles and Geomembranes*, vol. 36, pp. 44–54, 2013.

[55] VicRoads, *Crushed Rock for Light Duty Base and Subbase Pavement, Section 813*, VicRoads, Melbourne, Fla, USA, 2011.

[56] ASTM, "Standard test method for direct shear test of soils under consolidated drained conditions," ASTM D3080/D3080M, ASTM International, West Conshohocken, Pa, USA, 2011.